ISSN 1063-7826, Semiconductors, 2018, Vol. 52, No. 6, pp. 723–728. © Pleiades Publishing, Ltd., 2018.
Original Russian Text © N.M. Denisov, E.B. Chubenko, V.P. Bondarenko, V.E. Borisenko, 2018, published in Fizika i Tekhnika Poluprovodnikov, 2018, Vol. 52, No. 6, pp. 575–580.

SURFACES, INTERFACES, AND THIN FILMS

Optical Properties of Multilayered Sol–Gel Zinc-Oxide Films

N. M. Denisov, E. B. Chubenko*, V. P. Bondarenko, and V. E. Borisenko

Belarusian State University of Informatics and Radioelectronics, Minsk, 220013 Belarus

**e-mail: eugene.chubenko@gmail.com*

Submitted July 4, 2017; accepted for publication July 19, 2017

Abstract—Study of structural, optical and photocatalytic properties of multilayered (1–8 layers) zinc oxide films deposited on glass substrates by sol-gel method showed, that after thermal treatment at 500°C they consist of random oriented hexagonal crystalline grains with size of 34–40 nm, forming larger particles with sizes of 100–150 nm, which do not depend on number of layers. With an increase in the number of layers, the intensity of exciton photoluminescence decreases by a factor of 10, the absorption of light in the visible and near IR ranges increases, and the efficiency of photocatalytic decomposition of the test organic dye rhodamine B increases by 10–12%. The observed changes are related to the increase in the total area of grain boundaries and to the change in the integral amount of oxygen vacancies and interstitial atoms as the number of layers increases, which makes it possible to control the properties of zinc oxide films for applications in optoelectronics, photovoltaics and photocatalysis.

DOI: 10.1134/S1063782618060040

1. INTRODUCTION

Zinc oxide (ZnO) is a direct-gap II–VI oxide semiconductor with a band gap of 3.37 eV (at 300 K) and a large binding energy of excitons (60 meV) [1, 2], which allows the material to exhibit efficient exciton luminescence in the near-ultraviolet (UV) region even at room temperature and to transmit 80–90% of light in the visible range [1, 3]. Due to its physical, chemical, electronic, and optical properties, zinc oxide is considered to be a promising material for applications in optoelectronics and photovoltaics as well as for the production of photocatalytic coatings [1, 2, 4, 5].

The advantage of ZnO compared to other wide-gap semiconductors (GaN or AlN) is a possibility of producing nanostructures on the basis of this material by various methods, such as vapor phase deposition, chemical or electrochemical deposition, and sol–gel and hydrothermal synthesis [1, 6–8]. Among these methods, the sol–gel technology stands out due to optimal combination of the simplicity of implementation and low material costs with the possibility of repeatedly carrying out the process of the formation of nanostructured films in order to attain a required thickness of the whole film coating. However, the specific features of the structure and properties of such multilayered coatings remain poorly understood, and the data available in publications are contradictory [9–12].

Kaneva et al. [9] and Nozhinova et al. [10], who fabricated multilayered ZnO coatings (1–7 layers) by the sol–gel technique, noted that, the photocatalytic efficiency increased with the number of the layers. In [9, 10], this effect was attributed to an increase in the specific surface area. However, the study of the morphology and structure of such coatings [11, 12] showed that, as the number of layers was increased, the ZnO crystallite dimensions increased too, and it was assumed that, in contrast, the coating became more compact. At the same time, an increase in the conductivity of multilayered films was also observed [12, 13]. Therefore, it can be assumed that the above-mentioned growth of the photocatalytic efficiency can be associated not only with changes in the surface area, but with changes in the electronic and optical properties of the material within the multilayered coating as well.

The purpose of this study is to perform experimental investigation of the interrelation between changes in the structure, optical properties, and photocatalytic efficiency of multilayered ZnO films produced by the sol–gel method in relation to the number of sequentially deposited layers.

2. EXPERIMENTAL

Multilayered ZnO films were formed on 20 × 25 × 1 mm glass substrates by the sol–gel method in accordance with the previously developed procedure [14–16]. The substrate surfaces were preliminarily cleaned in acetone and distilled water. The sol used to deposit ZnO was a solution based on isopropyl alcohol (C_3H_7OH), monoethanolamine ($NH_2–CH_2CH_2–OH$), and anhydrous zinc acetate ($(CH_3COO)_2Zn$) in the

molar ratio 49:7:5. To form ZnO, the ready glass substrates were dipped into the sol for 1 min, after which they were slowly drawn out and dried in air at 200°C. In this manner, we deposited from one to eight layers, and then the whole multilayer structure was annealed in air at 500°C for 30 min.

The structure and phase composition of the multilayered films formed were studied by scanning electron microscopy (SEM) and X-ray diffraction (XRD) analysis, using a Hitachi S4200 microscope and a DRON-4 diffractometer ($\lambda = 1.54184$ Å), respectively.

Among the optical characteristics of the films, their reflectance and transmittance spectra as well as their photoluminescence (PL) spectra were studied at room temperature. The reflectance and transmittance spectra were recorded in the wavelength range from 200 to 1100 nm, using a Proscan MC-121 spectrophotometer. The PL signal was studied with a spectroscopy complex based on a Solar TII MS 7504i monochromator–spectrograph equipped with a Hamamatsu S7031-1006S silicon CCD matrix. The PL signal was excited with a 1 kW Xenon lamp; a monochromatic line with the wavelength of 345 nm was separated out from the emission spectra of the lamp, using a Solar TII DM 160 double monochromator.

The photocatalytic efficiency of the films was estimated from the decomposition of rhodamine B (Rh B) test organic dye in an aqueous solution upon exposure to ultraviolet light. To do this, we placed the experimental samples into Petri dishes with a solution of Rh B with the concentration 10 mg L^{-1} and kept them in the dark for 30 min to judge the role of adsorption of the dye in bleaching of the solution. Then the solution and the sample immersed into it were illuminated with light from a gas-discharge mercury lamp with a power of 8 W for 15 min; during illumination, the solution was constantly mixed. The lamp was equipped with a filter that separated a monochromatic line with the wavelength 365 nm. The concentration of the dye in the solution was determined from the intensity of the absorption band peak of Rh B at the wavelength 556 nm.

3. RESULTS

All obtained films have a white matt light-scattering surface typical to polycrystalline ZnO. Figure 1 shows SEM images illustrating the structure of the surface and the film itself in its cross section. Regardless of the number of layers, the films formed by the sol–gel technique possess a surface with a developed relief and consist of sphere-like particles of 100–150 nm in dimensions. In the case of a small number of layers (one or two), there also are rod-like particles at the surface, with the cross section close to a hexagon with a diagonal of about 150 nm and a length of up to 1 μm. They are lacking at the surface of the eight-layer film, and in addition, individual particles are arranged more closely to each other.

The developed surface relief of the films is responsible for a considerable variation of their thickness. Specifically, the thickness of one-, two-, and eight-layer films varies from 0.5 to 3 μm, from 1 to 4 μm, and from 7 to 7.4 μm, respectively.

According to the XRD data (Fig. 2), all of the films are polycrystalline in structure, with no pronounced prevalent orientation of grains. The set of diffraction peaks corresponds to crystalline ZnO with a hexagonal crystal lattice [1]. As the number of deposited layers increases, the intensity of the peaks increases, which is due to the larger amount of material synthesized. In the XRD spectra of one- and two-layer films, in the range of angles $2\theta = 20°–30°$, we observe a broad low-intensity band related to the glass substrate.

The crystallite dimensions calculated by the Debye–Scherrer formula are 34–40 nm for all presented crystallographic orientations of ZnO and do not depend on the number of deposited layers. These values are smaller than the particle dimensions determined from the SEM data. As calculated for one crystallographic orientation, the relation between the widths of XRD peaks (β) corresponding to different orders of reflection at the reflection angles θ_1 and θ_2 satisfies the condition $\beta_1\beta_2 = \cos(\theta_2)/\cos(\theta_1)$. This suggests that the experimentally observed broadening of diffraction peaks is defined exactly by small ZnO crystallites. Therefore, it is reasonable to conclude that the prevailing 100–150 nm particles observed by SEM (Fig. 1) are composed of 34–40 nm crystallites.

Figure 3 shows the transmittance and reflectance spectra of multilayered ZnO films. The films transmit light in the visible and near-infrared (IR) regions at a wavelength longer than 375 nm, i.e., at photon energies smaller than the band gap of the ZnO semiconductor. As the number of deposited layers is increased, the transparency of the films decreases exponentially, in accordance with the Buger–Lambert law. This suggests that the average film thickness increases linearly with increasing number of sol layers. As the number of sol layers is increased, the reflectivity of the films decreases as well, especially in the wavelength range from 550 to 1100 nm.

The surface with a developed relief causes the diffuse scattering of incident light, which is responsible for the lower transmittance and reflectance measured in the experiment (Figs. 3a, 3b). The optical transmittance observed for the films in the UV region of 300–380 nm is related to the PL signal detected by spectrophotometer from ZnO that emits light at longer wavelengths upon exposure to UV radiation.

From the transmittance and reflectance spectra of ZnO films, we calculated the absorption spectra in the

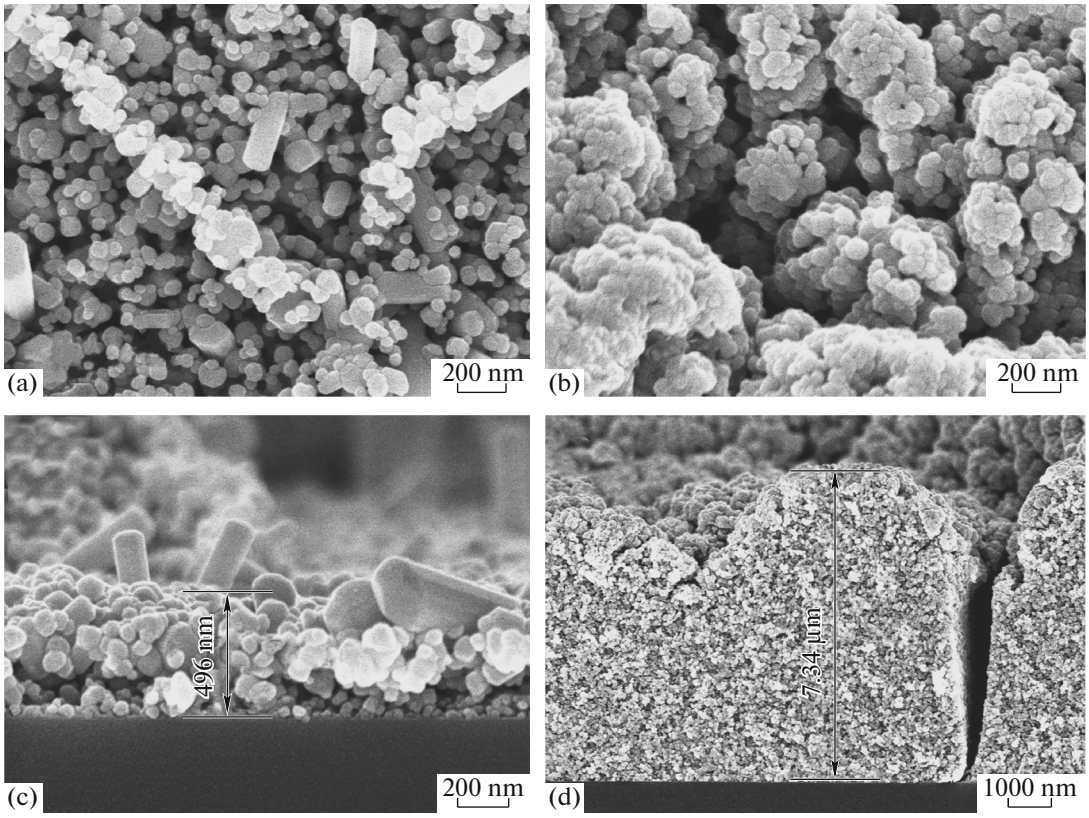

Fig. 1. (a, b) Surface and (c, d) cross section of the sol–gel derived ZnO films formed on glass substrates and consisting of (a, c) one and (b, d) eight sol layers.

Tauc's coordinates plots (Fig. 4). The optical band gap determined from the Tauc plots for ZnO at different numbers of layers is 3.15–3.20 eV, which is smaller than the band gap of single-crystal ZnO (3.34 –3.37 eV) [1, 2].

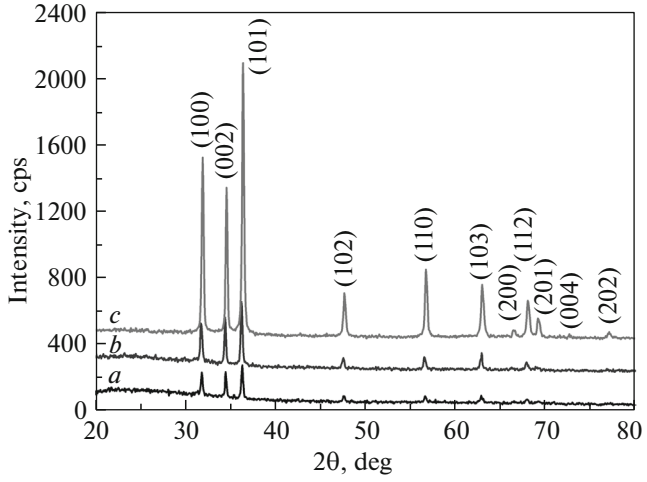

Fig. 2. XRD patterns of ZnO film samples with different numbers of the layers. The number of the layers is (a) one, (b) two, and (c) eight. Crystallographic planes of the hexagonal ZnO crystal lattice are indicated near the corresponding diffraction peaks.

The PL spectra of multilayered ZnO films (Fig. 5) show that the shape of the spectra substantially depends on the number of deposited layers. It should be noted that, in the spectrum of the single-layer structure, there are no PL bands related to the glass

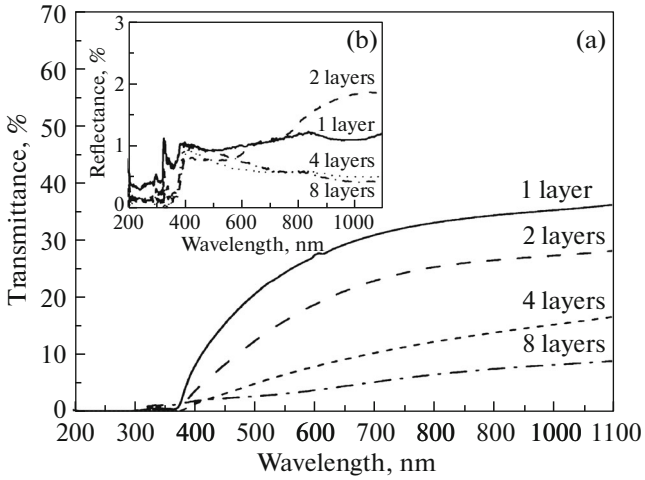

Fig. 3. (a) Transmittance and (b) reflectance spectra of ZnO films formed by the sol–gel method with different numbers of sequentially deposited layers.

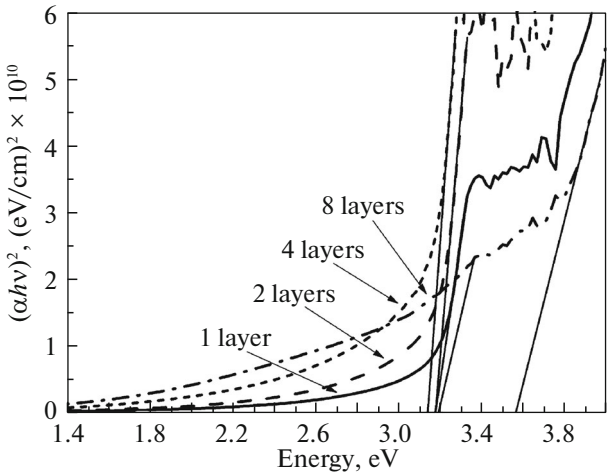

Fig. 4. Absorption spectra in Tauc coordinates for ZnO films consisting of different numbers of layers. Straight solid lines illustrate the extrapolation of the absorption edge to determine the band gap.

substrate. Thus, even in the case of the thinnest film among the samples fabricated in the study, the penetration depth of the excitation light (345 nm) is smaller than the film thickness. Consequently, the PL spectra correspond to emission from approximately the same volume of the material and can be directly compared with each other.

In the UV region of the PL spectra of all of the samples, we observe an asymmetric band, whose intensity decreases, as the number of layers is increased. This band consists of several different-order phonon replicas of the free-exciton line [17]. At room temperature, these replicas merge into one broad band because of temperature broadening. The maximum intensity is exhibited by a component corresponding to the one-longitudinal-phonon (1LO-phonon) replica, whose maximum is located in the energy region of 3.28 eV. Taking into account the exciton binding energy in ZnO (60 meV) [1, 2], we can estimate the band gap of ZnO is 3.34 eV. This value corresponds to the band gap of bulk ZnO [1, 2]. The above-mentioned narrower band gap determined from the absorption spectra is defined by blurring of the fundamental absorption edge because of the presence of defect levels in the band gap of ZnO [18].

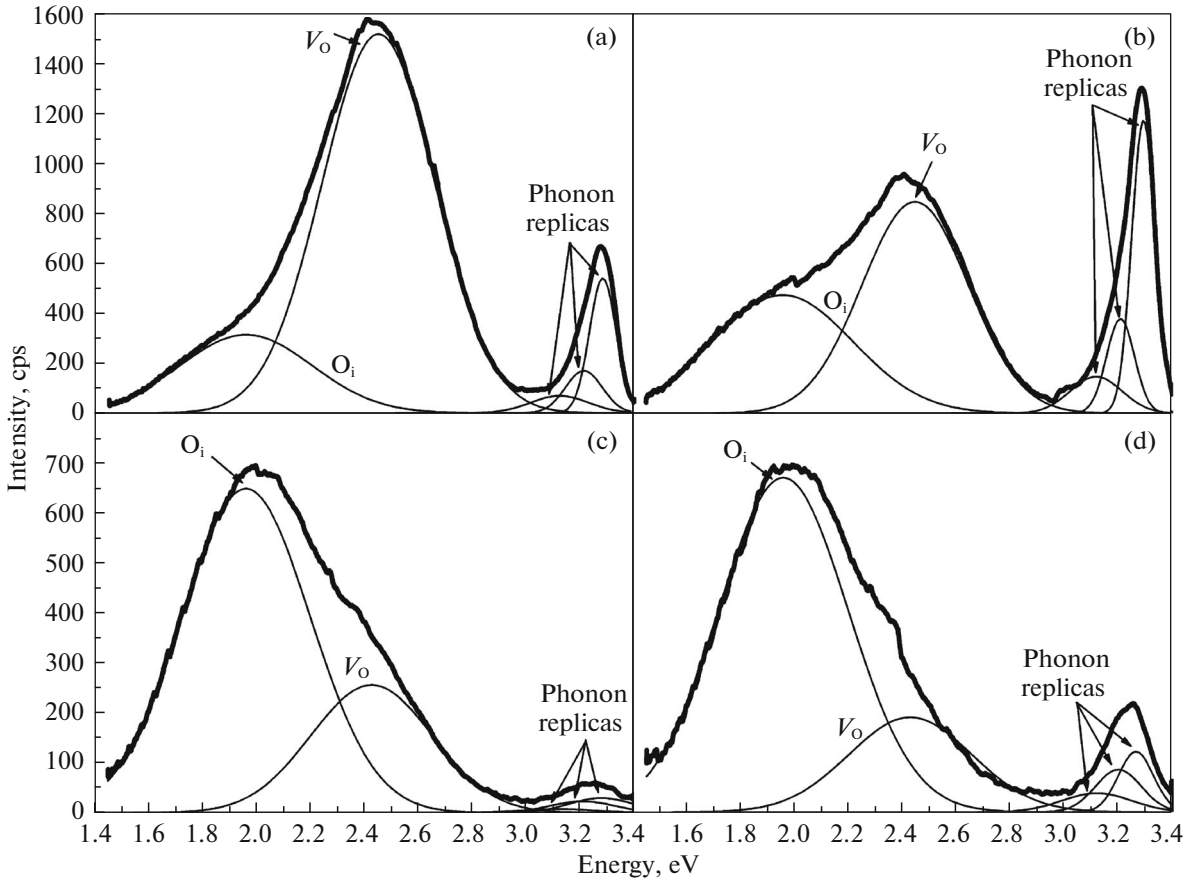

Fig. 5. PL spectra of sol–gel derived ZnO films consisting of different numbers of sequentially deposited layers. The number of layers is (a) one, (b) two, (c) four, and (d) eight.

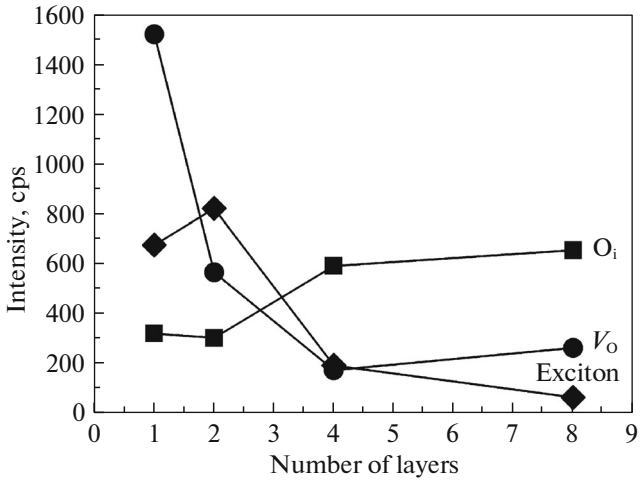

Fig. 6. Variations in the intensity of PL bands attributed to crystal-lattice defects (interstitial oxygen atoms O_i, oxygen vacancies V_O) and in the exciton PL intensity with increasing number of ZnO layers.

The PL band in the optical region of the spectrum exhibits a large spectral width (1.4–2.8 eV). As the number of ZnO layers is increased, the maximum of this band shifts to lower energies. Approximation of this band with symmetrical Gaussian functions shows that, for all of the samples, this band can be adequately fitted with two bands, whose maxima correspond to the photon energies of 1.96 and 2.45 eV. The 1.96-eV band is representative of the radiative transitions of charge carriers from the conduction band to band-gap levels defined by interstitial oxygen atoms (O_i) in ZnO [14], with subsequent nonradiative transitions to the valence band. Radiative transitions at an energy of about 2.45 eV involve oxygen vacancies (V_O) in the ZnO crystal lattice [19–21]. Thus, for samples with a large number of layers, the highest intensity is exhibited by the band related to O_i interstitial atoms. In this case, the exciton PL band in the near-UV region and the band related to V_O vacancy defects are quenched (Fig. 6).

Study of the photocatalytic efficiency of multilayered sol–gel ZnO films supports the previous observations of systematic features [9, 10] at a qualitative level. As the number of layers is increased, the efficiency of the photocatalytic decomposition of Rh B increases. For multilayered films, the efficiency is found to be 10–12% higher than that for single-layer films.

4. DISCUSSION

The blurred fundamental absorption edge and the well-pronounced Urbach tail in the transmittance spectra (Fig. 3a) suggest that the concentration of point defects in the structures is high. In the case of ZnO, the role of point defects is played by vacancies in the crystal lattice, interstitial oxygen and zinc atoms, and foreign impurity atoms incorporated into the crystal lattice of the semiconductor [1, 23]. The lower reflectance observed at long wavelengths of the optical region of the reflectance spectra (Fig. 3a), quenching of the exciton and defect-related PL signals (Fig. 6), and the strengthened Urbach tail for the samples with a larger number of layers can be attributed to the fact that the relief and structure of the film surface vary with the number of deposited layers. As the number of the layers is increased, the total number of defects responsible for nonradiative recombination and for the additional absorption of light becomes larger.

In the photocatalytic process, the efficiency of the decomposition of organic substances is defined by the number of photocatalyst surface centers, through which the electrons involved in redox reactions in the solution are transferred. The role of such centers is played by surface defects [24]. Since the multilayered ZnO films formed by the sol–gel method are structurally polycrystalline and exhibit a developed surface relief, the role of crystal-lattice defects at the crystallite surface is decisive. From variations in the optical and photocatalytic properties, the role of defects is visible, as the number of deposited layers is increased from one to four. The further increase in the number of layers does not result in the substantial modification of their properties.

5. CONCLUSIONS

The multilayered ZnO films formed by the sequential deposition of sol layers onto glassy substrates followed by subsequent heat treatment at 500°C are structurally polycrystalline, irrespective of the number of deposited layers. The structure is formed mainly by sphere-shaped 100–150 nm particles composed of ZnO crystallites of 34–40 nm in dimensions. The main optically active defects in the films are interstitial oxygen atoms and oxygen vacancies localized in the ZnO lattice near the crystallite surfaces. As follows from the behavior of the intensity of characteristic PL bands with increasing number of deposited layers, the total number of oxygen interstices increases, whereas the number of oxygen vacancies and annihilating exciton pairs decreases. At the same time, the photocatalytic efficiency of the multilayered films increases by 10–12%. This systematic feature is most pronounced, as the number of layers is increased from one to four. This can be used for controlling the optical and photocatalytic properties of multilayered ZnO coatings.

ACKNOWLEDGMENTS

The study was supported by the State Programs of Scientific Researches of the Republic of Belarus “Convergence”, project no. 3.2.04, and “Photonics,

Optoelectronics, and Microelectronics", projects no. 2.1.02.

We are grateful to D.V. Zhigulin for the SEM studies of experimental samples and to V.V. Uglov for XRD analysis of the samples.

REFERENCES

1. Ü. Özgür, Ya. I. Alivov, C. Liu, A. Teke, M. A. Reshchikov, S. Doğan, V. Avrutin, S.-J. Cho, and H. Morkoç, Appl. Phys. Rev. **98**, 041301 (2005).
2. A. Kolodziejczak-Radzimska and T. Jesionowski, Materials **7**, 2833 (2014).
3. A. Pimentel, E. Fortunato, A. Gonçalves, A. Marques, H. Águas, L. Pereira, I. Ferreira, and R. Martins, Thin Solid Films **487**, 212 (2005).
4. Ü. Özgür, D. Hofstetter, and H. Morkoc, Proc. IEEE **98**, 1255 (2010).
5. A. B. Djurišić, X. Chen, Y. H. Leung, and A. M. C. Ng, J. Mater. Chem. **22**, 6526 (2012).
6. L. Znaidi, Mater. Sci. Eng. B **174**, 18 (2010).
7. Z. Fan and J. G. Lu, J. Nanosci. Nanotechnol. **5**, 1 (2005).
8. M. Balucani, P. Nenzi, E. Chubenko, A. Klyshko, and V. Bondarenko, J. Nanopart. Res. **13**, 5985 (2011).
9. N. Kaneva, A. Bojinova, K. Papazova, D. Dimitrov, I. Svinyarov, and M. Bogdanov, Bulg. Chem. Commun. **47**, 395 (2015).
10. A. S. Bozhinova, N. V. Kaneva, I. E. Kononova, S. S. Nalimova, Sh. A. Syuleiman, K. I. Papazova, D. Ts. Dimitrov, V. A. Moshnikov, and E. I. Terukov, Semiconductors **47**, 1636 (2013).
11. H. Y. Bae and G. M. Choi, Sens. Actuators B **55**, 47 (1999).
12. T. Demes, C. Ternon, D. Riassetto, H. Roussel, L. Rapenne, I. Gélard, C. Jimenez, V. Stambouli, and M. Langlet, J. Phys. Chem. Solids **95**, 43 (2016).
13. M. I. Khan, K. A. Bhatti, R. Qindeel, N. Alonizan, and H. S. Althobaiti, Results Phys. **7**, 651 (2017).
14. N. M. Denisov, F. A. d'Avitaya, and V. E. Borisenko, Inorg. Mater. **50**, 572 (2014).
15. N. M. Denisov, A. V. Baglov, V. E. Borisenko, and E. V. Drozdova, Inorg. Mater. **52**, 523 (2016).
16. N. M. Denisov, A. V. Baglov, and V. E. Borisenko, Inorg. Mater. **53**, 176 (2017).
17. W. Shan, W. Walukiewicz, J. W. Ager III, K. M. Yu, H. B. Yuan, H. P. Xin, G. Cantwell, and J. J. Song, Appl. Phys. Lett. **86**, 191911 (2005).
18. V. Srikant and D. R. Clarke, J. Appl. Phys. **82**, 5447 (1998).
19. S. Vempati, J. Mitra, and P. Dawson, Nanoscale Res. Lett. **7**, 470 (2012).
20. B. Cao, W. Cai, and H. Zeng, Appl. Phys. Lett. **88**, 161101 (2006).
21. C. H. Ahn, Y. Y. Kim, D. C. Kim, S. C. Mohanta, and H. K. Cho, J. Appl. Phys. **105**, 013502 (2009).
22. S. Chakrabarti, D. Ganguli, and S. Chaudhuri, Mater. Lett. **58**, 3952 (2004).
23. A. Janotti and C. G. van de Walle, Rep. Prog. Phys. **72**, 126501 (2009).
24. K. M. Lee, C. W. Lai, K. S. Ngai, and J. C. Juan, Water Res. **88**, 428 (2016).

Translated by E. Smorgonskaya